Available online at www.sciencedirect.com
ScienceDirect
Forest Ecology and Management 244 (2007) 1–15
Forest Ecology and Management
www.elsevier.com/locate/foreco

A hierarchical approach for scaling forest inventory and fuels data from local to landscape scales in the Davis Mountains, Texas, USA

Helen M. Poulos [a,*], Ann E. Camp [a], Richard G. Gatewood [b], Lynn Loomis [c]

[a] Yale School of Forestry and Environmental Studies, 370 Prospect Street, New Haven, CT 06511, United States
[b] National Park Service, P.O. Box 368, Alpine, TX 79830, United States
[c] USDA Natural Resources Conservation Service, P.O. Box 1557, Marfa, TX 79843, United States

Received 14 July 2006; received in revised form 5 March 2007; accepted 12 March 2007

Abstract

This study combined hierarchical cluster analysis and classification and regression tree algorithms to quantify vegetation and fuel characteristics and to generate spatially explicit vegetation and fuels maps for forest and fire management in the Davis Mountains of west Texas, USA. We used field data, landscape metrics derived from digital elevation models, and spectral information from remotely sensed imagery to (1) determine recent changes in forest stand structure in relation to historical fire exclusion, (2) quantify the effects of fire exclusion on fuel accumulation patterns, and (3) develop predictive vegetation and fuels maps for our study area. Four vegetation types were identified by cluster analysis including: mesic woodlands, pinyon pine forests, alligator juniper forests, and gray oak forests. Vegetation types varied by elevation, landform type, potential relative radiation (PRR), and spectral signature. Age data suggested that the majority of pines in the Davis Mountains established near 1920, just after the widespread 1916 fire and favorable climatic conditions in 1919. Three fuel types were identified that also varied by elevation, landform type, PRR and spectral characteristics, although the importance of these variables in distinguishing fuel types differed from the environmental variables that discerned the vegetation types. Forest stand densities and fuel accumulations were high in the Davis Mountains, which was probably the result of fire exclusion from grazing activities beginning in the early 1900s. Results from this study will be used to implement forest and fire management activities directed toward ecosystem restoration and maintenance.

Keywords: Vegetation mapping; Fuels mapping; Gradient analysis; Classification and regression trees; Remote sensing; Forest stand structure

1. Introduction

Natural resource managers throughout the western United States need decision support tools to guide forest and fire management programs that focus on maintaining biodiversity and ecosystem function. Frequent, low intensity fire was a keystone ecosystem process in forests of the southwestern United States prior to fire exclusion from grazing beginning in the late 1800s and direct fire suppression that began in the early 1900s (Leopold, 1924; Faulk, 1970; Swetnam and Baisan, 1996). The removal of fire from the forested landscapes of the Southwest has stimulated a shift from historically open, park-like forests with little understory fuels to dense, stagnated forests with high live and dead fuel loads (Cooper, 1960; Biswell et al., 1973; Sackett, 1979; Harrington, 1982). Changes in the horizontal and vertical continuity of fuels have resulted in forest stand structures that are susceptible to intense crown fires that differ dramatically from the range of historical fire regime variability (USDA and USDI, 2000). The dramatic changes in recent fire behavior as a result of increases in the recruitment of vegetation and the accumulation of fuels in the absence of fire have triggered both public and private interest in reducing fuel loads and restoring forest stand structures to their range of historical natural variability through forest thinning and prescribed fire.

Managers need of a variety of tools to direct management prescriptions focused on reducing the risk of high intensity fire in regions that historically experienced frequent, low intensity fire. Baseline information about contemporary tree species composition, forest stand structure, and fuel accumulation patterns is an important first step in quantifying the changes that have occurred under fire suppression. However, this detailed

* Corresponding author. Tel.: +1 860 426 0266; fax: +1 203 432 3929.
E-mail address: helen.mills@yale.edu (H.M. Poulos).

0378-1127/$ – see front matter
doi:10.1016/j.foreco.2007.03.033

information is time consuming and costly to collect, and is therefore limited to a restricted number of sites in the Southwest (i.e. Fulé et al., 1997; Fulé et al., 2002; Moore et al., 2004; Heinlein et al., 2005).

A second step for informed forest and fuels management is the extrapolation of species-environment and fuels-environment relationships across landscapes through predictive mapping. Biophysical gradient modeling is a useful method for predicting plant species composition (Whittaker and Niering, 1965, 1968), forest stand structure (Ohmann and Spies, 1998), and fuel loads (Kessell, 1976; Keane et al., 1997, 2000; Falkowski et al., 2005) across landscapes of the western United States. However, the key environmental factors that control the abundance and distribution of vegetation and fuels vary between regions and across mountain ranges, signaling the need for site specific and spatially explicit information about landscape-scale variability in environmental site conditions and vegetation and fuel distribution patterns.

The combined use of detailed field-based vegetation and fuels data, environmental data, and satellite imagery is a promising method for accurate predictive mapping of vegetation and fuels (Keane et al., 2000, 2001; Ohmann and Gregory, 2002). Remotely sensed imagery offers an inexpensive and readily available form of ancillary data that has been used extensively for mapping vegetation and fuels. Alone, remotely sensed data of forest-covered areas are limited to the general characteristics of the upper forest canopy, which can lead to erroneous vegetation and fuel maps. However, forest inventory data, environmental data, and spectral information from remotely sensed satellite images can be used in suite to enhance the accuracy of vegetation and fuel maps.

This study used a hierarchical approach to characterize and model woody vegetation, forest stand structure, and fuel loads in the Davis Mountains Preserve of The Nature Conservancy (DMTNC) in the Davis Mountains of west Texas, USA. We used field-based data, biophysical gradient modeling, and remotely sensed imagery to characterize and scale tree species composition, forest stand structure, and fuel loads from the plot to the landscape scale. The goals of this study were to: (1) quantify forest distribution patterns and stand structure in relation to historical fire exclusion, (2) determine the effects of fire exclusion on fuel accumulation patterns, and (3) generate spatially explicit fuels and vegetation maps for use by forest and fire managers to identify high fire risk locations on the landscape for fuel reduction treatments via forest thinning and prescribed fire.

Vegetation and fuels mapping have been carried out successfully in selected regions of the western United States using a variety of techniques including: maximum likelihood classifiers (Miller et al., 2003), logistic regression (Brown, 1994), linear discriminant analysis (Lewis, 1998; Keane et al., 2000), kriging (Ohmann and Spies, 1998), most similar neighbor imputation (Moeur et al., 1999), gradient nearest neighbor imputation (Ohmann and Gregory, 2002; Ohmann et al., in press), artificial neural networks (Gopal and Woodcock, 1996), and classification and regression trees (Franklin, 1998, 2002; Falkowski et al., 2005). In recent years, classification and regression trees have proven to be robust techniques for mapping vegetation and fuels due to their non-parametric nature, ability to handle continuous and discrete data types, and capability to deal with missing data (Brown de Colstoun et al., 2003). In general, decision trees perform as well as or better than other classification methods, and the explicit structure of their output makes it easy to interpret the main factors that distinguish classes from one another. In light of the robust nature and flexibility of decision trees in handling a variety of data types, we employed a classification tree approach to scale our plot-level vegetation and fuels data across the landscape of DMTNC.

2. Study area

The Nature Conservancy Preserve of the Davis Mountains is located in Jeff Davis County in western Texas (Fig. 1). The Davis Mountains comprise the largest mountain range in Texas, spanning from 1524 to 2560 m in elevation. They form part of the northernmost extension of the Sierra Madre Oriental, which continues over 1500 km southward to the states of Puebla and Querétaro in Mexico. The Davis Mountains are 35–39 million years old, and originated in the same Eocene to Oligocene orogeny that formed most of the Front Range of the Rocky Mountains (Turner, 1977). Geologic substrates in DMTNC are derived from the erosional remnant of the once widespread Davis Mountains volcanic field. Consequently, the underlying rocks are predominantly extrusives, consisting of lavas and pyroclastics. Soils are generally shallow to moderately deep, and are volcanic in origin.

Vegetation of the Davis Mountains is composed of pinyon pine, juniper, oak and mixed conifer tree species. Dominant species include *Juniperus deppeana*, *Quercus grisea*, *Q. gravesii*, *Q. emoryi*, *Q. hypoleucoides*, *Pinus cembroides*, *P. strobiformis* and *P. Ponderosa*. Chihuahuan desert grasslands bound the site at lower elevations, while relict montane conifer forests form the upper elevational boundary (Hinckley, 1944).

The climate is arid, characterized by cool winters and warm summers. Mean annual precipitation is 400 mm in Ft. Davis,

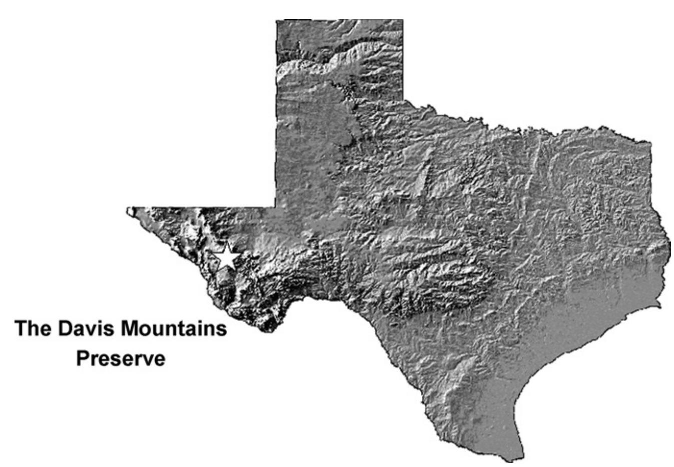

Fig. 1. Location of the Davis Mountains Preserve of The Nature Conservancy (DMTNC).

Texas, and is distributed bi-modally in late summer and winter with the majority of precipitation falling during summer monsoons (Bowmar, 1995). Mean monthly minimum temperatures range from 0.0 °C in January to 17.7 °C in July, while mean monthly maximum temperatures range from 15.5 °C in January to 32.6 °C in July.

3. Methods

3.1. Vegetation sampling

Two hundred and twenty-nine plots were established using a systematic sampling design. A grid was used to stratify sample plots at 600-m intervals across DMTNC at the intersection of grid lines to ensure that the plots captured the variability in local site conditions and tree species in the Davis Mountains. The spatial location of the center point of each plot was recorded using a global positioning system. Vegetation within each plot was sampled using nested, circular, fixed area plots All trees ≥5 cm diameter at breast height (dbh) were measured in 10 m in radius plots, and we recorded the species, dbh, total height, height at the base of the live crown, and the live crown ratio for each tree. Seedlings were tallied by species using 5 m radius plots. Plot areas were corrected for slope upon return from the field.

Forest stand structure was quantified using size, age, height, live crown height, and live crown ratio measurements. The density (ha^{-1}) of trees was calculated in 5 cm size-classes for each species in each plot as a measure of tree size structure. Stand age was determined by coring a subset of trees in each plot using an increment borer ($n = 430$). *P. cembroides*, *P. strobiformis*, and *P. ponderosa* were the only species sampled for the determination of stand age, because the majority of tree species in DMTNC do not produce annual growth rings making accurate age estimates difficult. Three seedlings (<5 cm dbh) were destructively sampled just outside the perimeter of each plot, and cross-sections were taken of each seedling at the base and at 30 cm high to determine the age of seedlings and to correct for the number of years lost at a coring height of 30 cm. Tree cores and seedling cross-sections were aged by sanding them to a high polish and visually cross-dating them under a binocular microscope using standard dendrochronological techniques (Stokes and Smiley, 1968). Additional years to the center were estimated with a pith locator (concentric circles matched to the curvature and density for the inner rings) for cores that missed the pith (Appelquist, 1958).

3.2. Fuels sampling

The fuels component of our study focused on the live canopy, standing dead, and dead and downed fuels in DMTNC. While we realize that fine fuel loads are major determinants of fire spread, we sampled only larger fuels to estimate locations on the landscape that were preconditioned to burn in high intensity fire events, or during extremely dry years (*sensu* Harrington, 1982). Our intent in sampling larger fuel particles was to generate information about the dominant topographic factors influencing the distribution of larger fuels at the landscape-scale.

The fuel loading of the forest canopy was quantified by taking a hemispherical photograph at the center point of each vegetation plot. Hemispherical photographs were taken with a Nikon Coolpix 900 digital camera with Coolpix 900 fish-eye lens mounted on a self-leveling tripod positioned 1 m above the ground. Pictures were taken under cloudy sky conditions in the morning. The leaf area index (LAI) of each plot was calculated using HemiView canopy analysis software version 2.1 (Delta-T Devices, 1999). LAI data were converted to crown bulk density (CBD) using the following equation derived by Keane et al. (2005):

$$\hat{y} = 0.0396 + 0.0511\,\mathrm{LAI}_{\mathrm{Hemiphoto}} \quad (1)$$

where $\hat{y}$ is the crown bulk density (kg m^{-3}) and $\mathrm{LAI}_{\mathrm{Hemiphoto}}$ is the LAI of the hemispherical photograph. The development of the CBD equation above was specifically designed for use with hemispherical photos. It was field tested in a wide range of forest types in the United States and should be applicable to the forests of DMTNC (Keane, personal communication).

Live fuel structure was determined by calculating the total basal area (BA) (ha^{-1}), and density (ha^{-1}) of trees in 5 cm size-classes in each sample plot. Standing dead tree structure was summarized by the total standing dead BA (ha^{-1}) and density (ha^{-1}) in 5 cm size-classes. The percent cover of grass and litter was estimated in six classes (<1%, 2–5%, 6–25%, 26–50%, 51–75%, and 76–100%).

Large dead and down fuels were sampled using the point relascope method for quantifying coarse woody debris (CWD) developed by Gove et al. (2001). Point relascope sampling (PRS) is a plotless sampling technique that is operationally efficient in the field, and compares closely to more traditional methods including fixed area and line intercept sampling for larger fuel particles (i.e. Brown, 1974; Brown et al., 1982) according to field tests by Brisette et al. (2003) and Jordan et al. (2004). As a plotless method that was superimposed on the circular vegetation plots, PRS was operationally more efficient in the field than traditional methods, especially in the extremely broken topography of DMTNC. PRS was carried out at the center point of each vegetation plot using a 28° angle of inclusion. The frequency (ha^{-1}), biomass (kg ha^{-1}), and volume (m^3 ha^{-1}) of larger fuels were calculated for 2.6–7.5 cm (100-h fuels) and >7.6 cm (1000-h fuels) time-lag fuel moisture categories only (Brown, 1974). Smaller fuel particles (<2.6 cm) were not sampled in this study. The time-lag is defined as the time period required for a fuel particle to reach ~63% of the difference between the initial moisture content and the equilibrium moisture content in a different environment (temperature, humidity). The 63% comes from the solution of a step response function and is given by $1 - 1/e = 0.63$ (Byram, 1963). This characteristic of the fuel particle is strongly correlated to its diameter, where the time-lag period was estimated by measuring the particles' diameter (Fosberg and Deeming, 1971). Species-specific values for the specific gravity of downed fuels were taken from Brown et al. (1982) for conifers and Maingi and Ffolliot (1992) for oaks.

3.3. Classification

Hierarchical cluster analysis using relative Euclidean distances and Ward's method was used to identify vegetation and fuel types in DMTNC based upon the good performance of the relative Euclidean distance metric and Ward's linkage method on ecological datasets (McCune and Grace, 2002). We identified the major vegetation types in DMTNC by clustering species importance values for each vegetation sample plot. Species importance values were calculated as percentages using the sum of the relative density and the relative BA of each species (0–200 range). Fuel types were determined by clustering the CBD, total live and standing dead BA, live and dead tree density, and the density, volume, and biomass of 10, 100, and 1000 h dead and downed fuels. Variable values were standardized to *z*-scores before clustering to account for differences in means and variances.

Indicator species analysis (Dufrêne and Legendre, 1997) with Euclidean distances as the distance metric was used to determine the significant indicator species in each vegetation type. Indicator species analysis combines information on the concentration of species abundance in a particular group and the faithfulness of occurrence of a species in a particular group, where a perfect indicator always appears in that group (McCune and Grace, 2002). The significance of indicator values is tested using a Monte Carlo randomization approach. Cluster analysis and indicator species analysis were preformed using PC-Ord software (McCune and Mefford, 1999).

Significant differences in fuel characteristics and environmental variables among vegetation and fuel types were identified using Kruskal–Wallis (Kruskal and Wallis, 1952) tests using Minitab, Version 12.2 statistical software (Minitab, 1999). A non-parametric test was chosen for this analysis in light of the non-normal distribution of the environmental data.

3.4. Landscape metrics

A set of 12 raster-based topographic, landform, and solar radiation variables were derived using the National Elevation Dataset (NED) for the study area at a 30 m $\times$ 30 m spatial resolution (USGS, 2005) (Table 1). We filtered each of these grids using a 3 by 3 pixel window assigning the mean value to the center pixel to reduce fine scale noise in the dataset. Raster values for the landscape metrics were assigned to each plot by intersecting the spatial location of the sample plot with each landscape data layer using ArcMap 9.2 software (ESRI, 2005).

3.5. Landsat 7 ETM+

A cloudless Landsat enhanced Thematic Mapper (ETM+) image from 18 June 2002 was used to develop six independent data layers from bands 1–5 and 7. A June scene from 2002 was chosen because it coincided with the timing of field sampling of vegetation and fuels, and because the scene was taken just prior to the onset of the summer monsoon. All tree species in the study area are evergreen, and therefore a summer scene was chosen to reduce the noise in the spectral signature from winter perennial grasses and herbaceous vegetation. We transformed the image into tasseled cap brightness, greenness, and wetness indices (Kauth and Thomas, 1976), and computed a soil adjusted vegetation index (SAVI) (Gilabert et al., 2002). SAVI was chosen over the more widespread normalized difference vegetation index (NDVI) in light of its poor performance in arid regions (Huete, 1988). The raster grids were filtered in the same manner as the landscape grids, and ETM+ derived values were also assigned to vegetation and fuel plots by intersecting the spatial location of the plots with each of the satellite data layers in succession. Significant differences in landscape and spectral data among vegetation and fuel types were determined using Kruskal–Wallis tests.

Table 1
Explanatory variables used for decision tree construction and mapping of vegetation types and fuel characteristics in DMTNC

Variable code	Definition
Landscape metrics	
Elevation	Elevation (m), from 30-m digital elevation model (DEM)
N aspect	Cosine transformation of aspect (°) (Beers et al., 1966) 1.0 (southwest) to −1.0 northeast
S aspect	Sine transformation of aspect (°) (Beers et al., 1966) 1.0 (southwest) to −1.0 northeast
Slope	Slope (°), from 30-m DEM
PRR	Cumulative potential relative radiation based on hourly solar position, topography and topographic shading (Pierce et al., 2005)
Topopos 150	Topographic position, calculated as the difference between a cell's elevation and the mean elevation of cells within a 150 m radius
Topopos 450	Topographic position, calculated as the difference between a cell's elevation and the mean elevation of cells within a 450 m radius
Topo configuration	Topographic configuration ranging from concave to convex calculated using the spatial analyst function in ArcMap 9.1
Landform	Landform type derived from a fuzzy-kmeans classification of elevation, relative elevation, plane curvature, stream power index profile curvature, slope gradient, compound topographic index, and flow accumulation derived from 30-m DEM using FuzME software (Minasny and McBratney, 1999)
Flow direction	Flow direction from ArcHydro extension in ArcMap 9.1 and 30-m DEM
Landsat ETM+	
Band 1	Band 1 (blue)
Band 2	Band 2 (green)
Band 3	Band 3 (red)
Band 4	Band 4 (near-infrared)
Band 5	Band 5 (mid-infrared)
Band 7	Band 7 (mid-infrared)
Brightness	Soil brightness index from tasseled cap transformation
Greeness	Green vegetation index from tasseled cap transformation
Wetness	Wetness index from tasseled cap transformation
SAVI	Soil adjusted vegetation index (Gilabert et al., 2002)

3.6. Predictive mapping

The two most common methods for mapping fuels are direct and indirect remote sensing (*sensu* Keane et al., 2001). Direct remote sensing is the mapping of fuels directly from remotely sensed satellite imagery. This method is simple and straight forward, but is often associated with significant error. Dead and down fuels are often not captured by the majority of remote sensors because they fail to penetrate the forest canopy (Belward et al., 1994). Thus, the classification of fuels using remotely sensed imagery alone is actually based on the spectral signature of the vegetation, rather than the spectral signature of the fuels in question. The second approach, indirect remote sensing, maps vegetation first using satellite imagery, and then assigns fuel types to the different vegetation types. This method assumes that vegetation characteristics correlate well with fuel characteristics, and that vegetation properties can be used to describe differences in fuel types. The major disadvantage of this approach is that stand history, biophysical setting, and forest stand structure can have major influences on the distribution of fuels. A particular vegetation type may display a wide range of fuel loads depending on its spatial location, stand age, and disturbance history. In light of the potential errors associated with direct and indirect fuels mapping, we mapped vegetation and fuels separately to minimize the errors associated with using vegetation properties as a surrogate for direct fuels mapping.

We used classification trees (Breiman et al., 1984) to generate spatially explicit maps of vegetation and fuels in DMTNC by using landscape metric and spectral data to scale the vegetation and fuels types we identified by cluster analysis from the plot- to the landscape-scale. Classification and regression trees (CART) belong to a family of algorithmic methods that generate decision trees from a set of learning cases. Recursive partitioning searches through the landscape metric and spectral data to find the greatest separation between pre-defined vegetation types and fuel types (determined from cluster analysis). Classification trees are ideal for mapping ecological datasets because they are non-parametric, can handle categorical variables, and are robust to outliers (De'ath and Fabricius, 2000). Furthermore, their output is easy to interpret and the decision rules created through classification trees can be linked to environmental processes across landscapes.

Vegetation and fuel decision trees were constructed using the rpart package in the statistical language R (R Development Core Team, 2005). The rpart package implements a recursive-partitioning algorithm that parallels the classification tree methodology of Breiman et al. (1984). The final vegetation and fuel maps were produced using Decision Tree in ENVI remote sensing software, version 4.2 (Research Systems Inc., 2005).

3.7. Model fitting

The fits of the vegetation and fuel models were evaluated by examining the cost-complexity parameters which measure how well the explanatory landscape metric and Landsat ETM+ derived variables separate the data. Traditionally, a tree is grown that overfits the model so that all the training data are correctly classified. A 10-fold cross-validation procedure corrects this overfitting by evaluating each node of the initial decision tree in terms of the classification error rate on the training set using a cost-complexity function (Breiman et al., 1984). The best model size is determined by selecting the tree that is within one standard deviation of the minimum misclassification error. Finally, the test dataset is used to determine overall model performance.

3.8. Classification accuracy

The percentage of misclassification and the Kappa statistic (Congalton and Green, 1999) were used as measures of classification accuracy for the two different models. The Kappa statistic, which ranges between 0 and 1, is a measure of the difference between the actual correct classification of the data and the correct classification of the data by chance alone. A Kappa of 0.60 therefore means that the classification accuracy was 60% greater than chance.

We tested the accuracy of the classification tree models by generating vegetation and fuel models using an 80% subset of randomly selected data to construct the models, and reserving 20% of the data for model validation. This process was repeated 1000 times using random subsets of the data without replacement as an estimate of overall model performance.

Field validation of the two models was carried out to assess map accuracies ($n = 100$). Validation points were stratified in the field by vegetation type and fuel type. The accuracy of the vegetation map was assessed through visual estimates of % cover of dominant tree species in six cover classes (<1, 1–4%, 5–24%, 25–49%, 50–74%, and 75–100% cover). The accuracy of the fuel map was assessed using point relascope sampling (Gove et al., 2001).

4. Results

4.1. Vegetation types and forest stand structure

Four vegetation types were identified using cluster analysis and mapped via recursive partitioning: (1) pinyon pine (*P. cembroides*) forests (PP), (2) gray oak (*Q. grisea*) forests (GO), (3) alligator juniper (*J. deppeana*) forests (AJ), and (4) mesic woodlands (MW) (Fig. 2). Indicator species varied by vegetation type (Tables 2 and 3), and the spatial distribution of vegetation differed significantly by topography (landscape metrics) and spectral signature (Landsat ETM+ data) (Table 4, Fig. 3).

All vegetation types had high densities of young, small diameter trees (Table 5, Fig. 4). All conifer species had reverse-J size class distributions suggesting an all age structure, while gray oak showed a peak at intermediate size classes (10–15 cm dbh). Forest age distributions were uneven-aged, and were dominated by relatively young trees that established near 1920 (Fig. 5), just after the last widespread fire in DMTNC (Poulos, unpublished data).

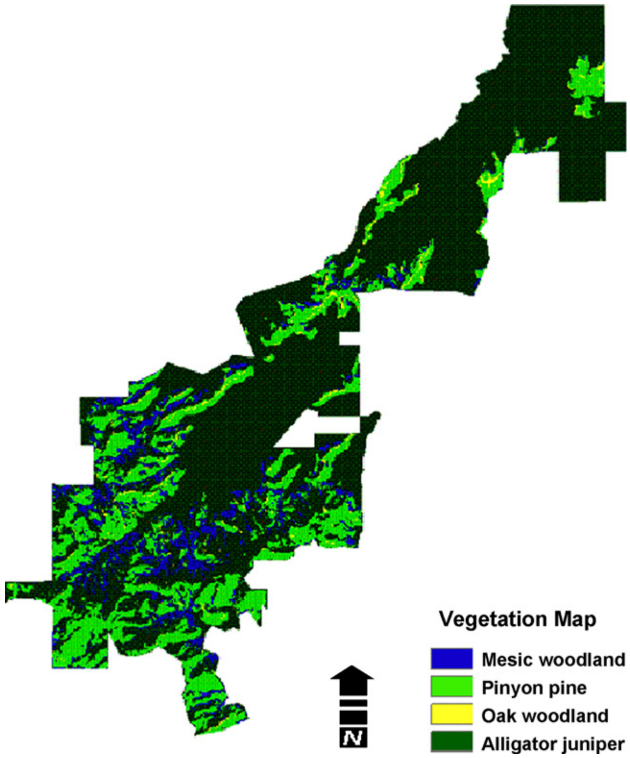

Fig. 2. Vegetation map for the Davis Mountains Preserve (DMTNC) developed using recursive partitioning. Vegetation types (gray oak, alligator juniper, pinyon pine, and mesic woodland) were determined using cluster analysis of species importance values.

4.2. Pinyon pine forests

P. cembroides was the most important indicator species in this vegetation type (Tables 2 and 3). The PP vegetation type existed at middle and upper elevations (1750–2400 m) on convex, upper topographic positions with steep slopes, with high runoff (sediment flow) (Table 4, Fig. 3). Band 7 (mid-infrared), slope, and potential relative radiation (PRR) were the most important predictors of the PP forest type from recursive partitioning (Fig. 3). PP forests were the oldest stands in DMTNC (mean = 93.3 years), and had the lowest basal area (11.4 m^2 ha^{-1}). This forest type had high densities of small *P. cembroides*, mixed with scattered, small *J. deppeana*, *Q. grisea*, and *Q. emoryi* (Table 2, Fig. 4).

4.3. Gray oak forests

Q. grisea was the most important indicator species in the GO forest type, with *Q. hypoleucoides*, *P. cembroides* and *J. deppeana* also present as minor associated tree species (Tables 2 and 3). The GO vegetation type was found at middle and upper elevations (1900–2400 m) on convex, upper topographic positions with steep slopes and high PRR (Table 4). Recursive partitioning separated this group by slope and PRR (Fig. 3). The GO vegetation type displayed characteristics typical of an oak savanna woodland, and was the most sparsely vegetated forest cover type in DMTNC. GO forests had low densities of scattered, short-stature *Q. grisea*, *Q. hypoleucoides*, *P. cembroides*, and *J. deppeana*. Intermediate sized (10–15 cm dbh) *Q. grisea* composed the forest overstory,

Table 2
Mean importance values (IV), density (ha^{-1}), basal area (BA) (ha^{-1}), stand age (years), # forest strata, crown height (m), live crown ratio # age cohorts, stand height (m), and live crown height for vegetation types in the Davis Mountains (DMTNC)

Vegetation type	Oak–pinyon–juniper (n = 49)			Pinyon pine (n = 73)			Gray oak (n = 26)			Alligator juniper (n = 66)			Mesic woodland (n = 15)		
	IV	BA	Density	IV	BA	Density	IV	BA	Density	IV	BA	Density	IV	BA	Density
Arbutus xalapensis	0.0	0.0	0.0	0.1	0.0	1.8	0.0	0.0	7.7	0.1	0.0	0.0	2.9	0.0	79.0
Juniperus deppeana	55.8	6.2	379.6	21.4	2.0	148.2	8.5	0.0	103.4	129.8	9.1	703.2	21.9	2.6	175.0
Pinus cembroides	45.9	3.6	458.1	109.2	5.7	643.6	22.9	1.4	134.5	38.2	1.8	299.6	18.7	1.1	180.5
Pinus ponderosa	1.6	0.0	13.3	0.6	0.0	2.2	1.0	0.0	4.7	1.2	0.0	44.4	30.6	3.6	199.2
Pinus strobiformis	0.0	0.0	0.0	0.0	0.0	0.0	0.0	0.0	0.0	0.0	0.0	0.0	12.7	0.7	91.2
Quercus emoryi	0.6	0.0	32.9	4.4	0.0	71.2	0.5	0.0	25.2	1.5	0.0	164.7	20.2	0.6	131.7
Quercus gambellii	0.3	0.0	2.3	0.0	0.0	14.3	0.0	0.0	2.2	0.0	0.0	2.6	21.6	0.9	111.7
Quercus gracilliformis	0.0	0.0	0.0	0.0	0.0	0.0	0.0	0.0	0.0	0.0	0.0	0.0	12.0	0.0	43.0
Quercus gravesii	0.6	0.0	2.6	0.1	0.0	2.8	2.0	0.0	7.7	0.0	0.0	12.1	7.6	1.2	80.0
Quercus grisea	52.2	7.3	458.9	30.9	3.8	282.3	82.4	9.6	537.2	12.4	2.5	219.4	13.6	3.2	117.6
Quercus hypoleucoides	42.7	1.0	24.1	3.1	0.0	7.5	83.6	1.0	60.0	16.6	0.0	52.7	27.7	0.0	604.7
Quercus shumardii	0.0	0.0	0.0	1.0	0.0	2.8	0.0	0.0	0.0	0.0	0.0	0.0	0.7	0.0	0.0
Quercus oblongifolia	0.0	0.0	0.0	0.4	0.0	0.0	0.0	0.0	0.0	0.0	0.0	0.0	1.0	0.0	3.7
Total	200.0	18.1	1371.9	200.0	11.4	1176.6	200.0	12.0	882.5	200.0	13.4	1498.8	200.0	14.0	1817.4
Stand age (years)		80.4			93.3			84.3			78.6			80.4	
# Strata		3			3			2			3			3	
# Age cohorts		2			1			1			1			1	
Stand height (m)		4.4			4.4			3.5			4.5			5.6	
Live crown height (m)		1.2			1.2			0.9			1.2			1.8	
Live crown ratio		0.3			0.3			0.3			0.3			0.3	

Vegetation types were determined from cluster analysis using relative Euclidean distances and Ward's method for plots in DMTNC (n = 229). Cluster dendrogram pruned and vegetation types determined using indicator species analysis (Table 3).

Table 3
Indicator values (% of perfect indication) of each species from indicator species analysis for vegetation types in the Davis Mountains Protected Area (DMTNC) using Euclidean distances

Species	Pinyon pine ($n = 73$)	Gray oak ($n = 26$)	Alligator juniper ($n = 66$)	Mesic woodland ($n = 64$)	p-Value
Arbutus xalapensis	0	1	0	5	0.135
Juniperus deppeana	8	5	54	23	**0.001**
Pinus cembroides	43	7	16	21	**0.001**
Pinus ponderosa	0	0	2	12	**0.048**
Pinus strobiformis	0	0	0	5	**0.049**
Quercus emoryi	6	1	11	3	0.469
Quercus gambelii	6	0	0	7	0.354
Quercus gracilliformis	0	0	0	6	0.067
Quercus gravesii	0	1	0	3	0.415
Quercus ghsea	18	38	11	24	**0.001**
Quercus hypoleucoides	0	2	1	10	0.065
Quercus oblongifolia	2	0	0	1	0.635
Quercus shumardii	1	0	0	0	1

Significant indicator species ($p \geq 0.05$) are indicated in bold, and were determined by a Monte Carlo test of significance of the observed maximum indicator value for each species, based on 1000 randomizations.

with the other species present in the understory as seedlings (0–5 cm dbh) (Table 2, Fig. 4).

4.4. Alligator juniper forests

Alligator juniper forests were the dominant low elevation vegetation type. *J. deppeana* was the major indicator species in this vegetation type (Table 3), with *P. cembroides* and oak species including *Q. grisea*, *Q. emoryi*, *Q. hypoleucoides* present as minor associates. The AJ vegetation type was found at low elevations (<1900 m), and at higher elevations on canyon walls, back slopes, and middle to upper elevation crests (Fig. 3). This vegetation type dominated lower topographic positions with gentle slopes, high PRR, and high runoff (Table 4). Elevation, landform type, and band 7 (mid-infrared) were the most important predictor variables for this vegetation type based on recursive partitioning (Fig. 3). AJ stands had high densities of *J. deppeana* and *P. cembroides* across size-classes ranging from 0 to 25 cm dbh, and lower densities of small oaks (0–5 cm dbh) in the understory (Table 2, Fig. 4).

Table 4
Mean predictor variables for the vegetation types determined by cluster analysis of species importance values in the Davis Mountains Protected Area (DMTNC)

	Vegetation type			
	Pinyon pine ($n = 73$)	Gray oak ($n = 26$)	Alligator juniper ($n = 66$)	Mesic woodland ($n = 64$)
Elevation***	2025 ± 188.3	2050 ± 15.2	1800 ± 26.7	2000 ± 14.9
Topopos_450**	6.8 ± 3.9	5.3 ± 3.1	−3.0 ± 6.0	−8.2 ± 3.2
Topopos_150*	1.9 ± 1.2	0.0 ± 1.0	−0.5 ± 1.8	−1.3 ± 0.8
Slope***	19 ± 1.3	20 ± 1.2	11 ± 2.1	16 ± 0.9
PRR**	19558 ± 551.8	20266 ± 297.4	20133 ± 411.8	18500 ± 206.4
N flow direction**	0.6 ± 4.1	−0.1 ± 3.4	0.5 ± 6.3	0.6 ± 4.6
S flow direction**	1.0 ± 13.2	0.8 ± 10.2	1.0 ± 17.0	1.0 ± 13.1
Flow accumulation*	14 ± 4.1	24 ± 3.4	41 ± 6.3	105 ± 4.6
Topo configuration*	0.20 ± 1.3	0.23 ± 1.1	0.00 ± 1.9	−0.11 ± 0.8
Sediment flow*	34 ± 0.9	18 ± 0.8	26 ± 1.6	11 ± 0.8
N aspect	−0.08 ± 0.0	0.02 ± 0.0	0.09 ± 0.0	0.09 ± 0.1
S aspect	−0.10 ± 0.0	−0.07 ± 0.2	−0.04 ± 0.4	−0.03 ± 0.0
Band 1***	92 ± 5.3	116 ± 4.8	101 ± 7.4	83 ± 4.2
Band 2***	92 ± 5.5	116 ± 5.6	101 ± 8.1	83 ± 4.6
Band 3***	81 ± 6.2	102 ± 5.8	90 ± 9.7	72 ± 4.2
Band 4*	143 ± 6.1	175 ± 5.7	144 ± 8.9	143 ± 4.6
Band 5***	105 ± 12.0	134 ± 8.7	125 ± 24.1	100 ± 2.9
Band 7***	85 ± 5.4	106 ± 5.6	102 ± 8.0	78 ± 4.1
Brightness***	194 ± 6.0	212 ± .5.2	206 ± 9.2	191 ± 4.9
Greeness***	−43 ± 6.3	−49 ± 5.2	−48 ± 8.5	−40 ± 5.0
Wetness***	−41 ± 5.5	−50 ± 5.3	−51 ± 7.9	−42 ± 4.0
SAVI***	−0.142 ± 0.8	−0.189 ± .0.9	−0.193 ± 1.4	−0.115 ± 0.8

Asterisks (*) next to the variable name denote significant differences in values between groups according to Kruskal–Wallis tests, with * indicating significance at the $p < 0.05$, ** indicating significance at $p < 0.01$, and *** indicating significance at $p \leq 0.001$.

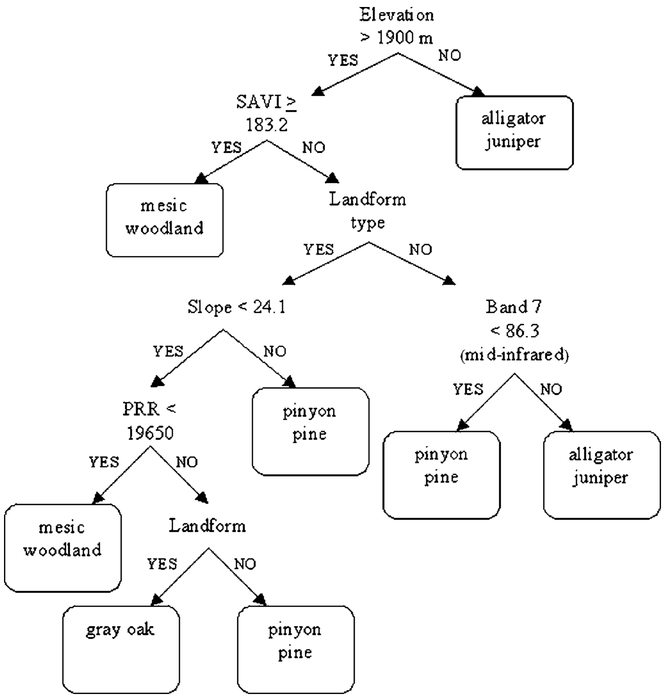

Fig. 3. Classification tree decision rules for fuel types in DMTNC. Vegetation types were determined using hierarchical cluster analysis of species importance values.

4.5. Mesic woodlands

The MW vegetation type had the highest species richness of any vegetation type (Table 2), and was mainly dominated by mixed conifer forest species. Mesophytic tree species including *P. strobiformis*, *P. ponderosa*, *P. cembroides*, and *J. deppeana* were important indicator species in this forest cover type (Tables 2 and 3). MW stands were found at middle and upper elevations (1770–2330 m) in valley bottoms, with gentle slopes, low PRR, low sediment flow and high flow accumulation (Table 4). MW had the highest greenness, wetness, and SAVI values of all vegetation types. SAVI was the most important predictor of this vegetation type. Recursive partitioning separated this group by SAVI, slope, and PRR (Fig. 3). MW also had the highest stand height (5.6 m), live crown height (1.8 m), tree basal area (14 m^2 ha^{-1}) and tree density (1817 ha^{-1}) of all forest cover types. MW stands had high densities of *Q. hypoleucoides*, and lower densities of other tree associates in the understory. Lower densities of *P. ponderosa*, *P. strobiformis*, and *Q. grisea* comprised the forest overstory (Table 2, Fig. 4).

4.6. Fuel types

Three fuel types were identified using cluster analysis and mapped via recursive partitioning (Figs. 6 and 7). Fuel types

Table 5
Mean ± S.E. values of fuel characteristics for fuel types in DMTNC determined from cluster analysis of fuel variables using relative Euclidean distances and Ward's method

	Fuel type		
	1 ($n = 91$)	2 ($n = 59$)	3 ($n = 79$)
Fuel characteristics			
Crown bulk density (kg m^{-3})*	0.093 ± 0.025	0.071 ± 0.002	0.069 ± 0.002
100-h (kg ha^{-1})*	1913 ± 227.1 (0.860)	4342 ± 30.8 (1.953)	2534 ± 28.9 (1.140)
1000-h (kg ha^{-1})*	7910 ± 592.3 (3.566)	6340 ± 10.5 (2.853)	10783 ± 182.6 (4.852)
Logs (ha^{-1})*	77 ± 366.0	11 ± 7.0	89 ± 24.8
Volume (m^3 ha^{-1})*	4 ± 42.3	1 ± 3.0	14 ± 10.5
Live BA (m^2 ha^{-1})*	18 ± 8.1	10 ± 0.8	11 ± 0.8
Standing dead BA (m^2 ha^{-1})	2.3 ± 4.4	1.7 ± 0.3	2.1 ± 0.3
Grass cover (%)	59 ± 15.6	58 ± 2.5	56 ± 2.3
Shrub cover (%)*	24 ± 18.3	18 ± 1.3	25 ± 2.0
Litter cover (%)*	57 ± 16.9	45 ± 2.8	48 ± 2.1
Standing dead trees (ha^{-1})			
5–10 cm	0 ± 0.0	0 ± 0.0	0 ± 0.0
10–15 cm	0 ± 0.0	0 ± 0.0	1 ± 0.0
15–20 cm	0 ± 0.0	0 ± 0.0	0 ± 0.0
20–25 cm**	41 ± 69.8	25 ± 8.5	24 ± 4.4
Live trees (ha^{-1})			
0–5 cm*	1242 ± 1279.6	157 ± 23.8	353 ± 43.8
5–10 cm*	357 ± 321.3	81 ± 12.0	131 ± 18.8
10–15 cm*	340 ± 224.4	114 ± 14.4	171 ± 19.0
15–20 cm*	170 ± 100.0	82 ± 9.5	108 ± 9.4
20–25 cm**	72 ± 53.6	47 ± 5.9	47 ± 4.3
25–30 cm	23 ± 24.0	23 ± 4.3	22 ± 3.1
30–35 cm	13 ± 20.0	12 ± 2.5	11 ± 1.9
35–40 cm	5 ± 13.1	3 ± 1.2	4 ± 1.5
>40 cm*	4 ± 13.0	9 ± 0.8	14 ± 1.4

Fuel loads of the fuel types are listed in tonnes/acre in parentheses. Asterisks (*) next to the variable name denote significant differences in values between groups according to Kruskal–Wallis tests, with * indicating significance at the $p < 0.05$ and ** indicating significance at $p < 0.01$.

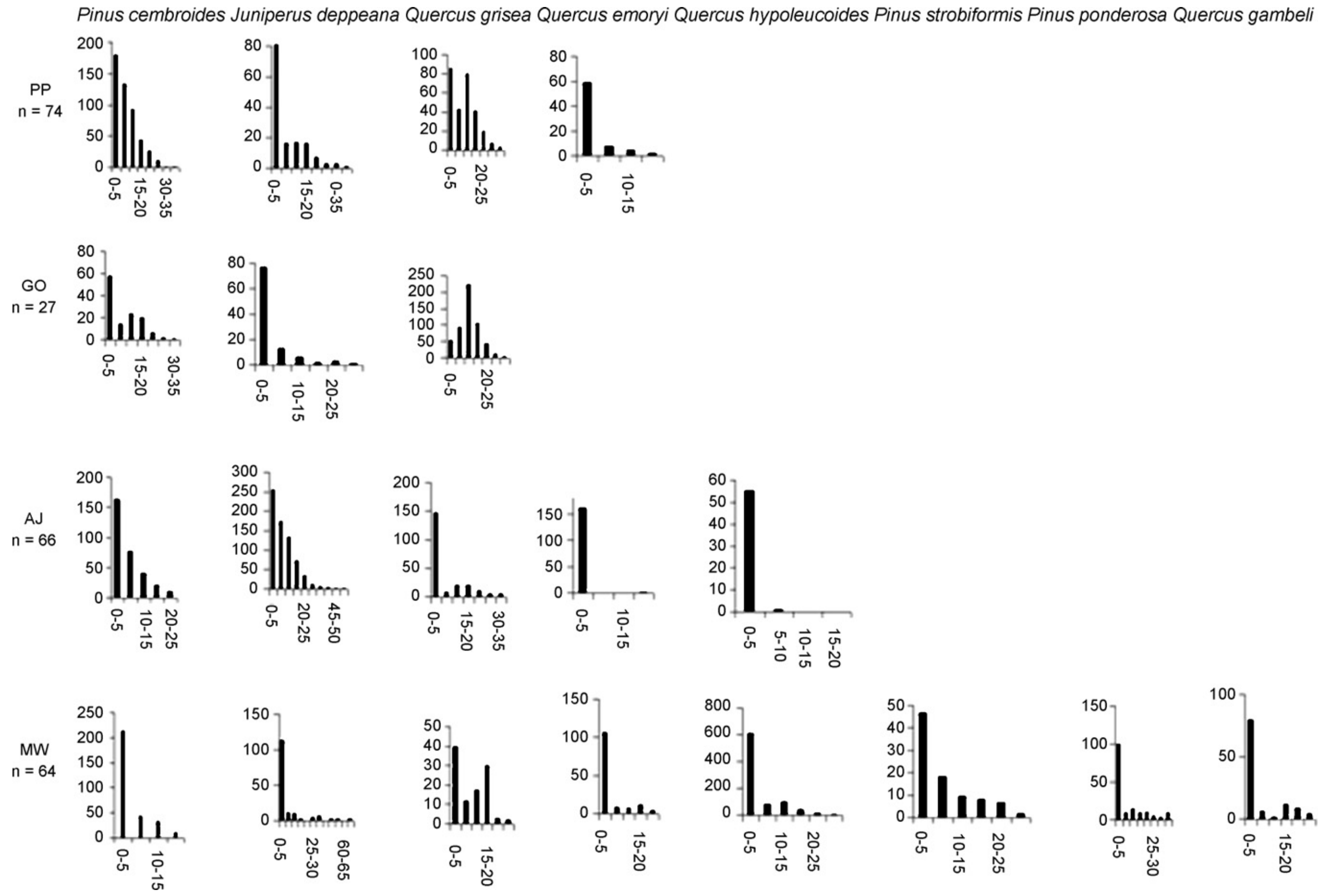

Fig. 4. Size-class distributions (# ha^{-1}) of tree species in 5 cm size-classes for vegetation types in DMTNC determined using cluster analysis. The *x*-axis represents size class, and the *y*-axis represents the # trees per ha. Note that the scale of the *y*-axis differs between graphs.

varied significantly by fuel characteristics in DMTNC (Table 5), topography (landscape metrics), and spectral signature (Landsat ETM+ data) (Table 6, Fig. 7). PRR, brightness, greenness, wetness, SAVI, and mid-infrared reflectance (band 7) were the most important predictor variables for determining fuel loadings in DMTNC (Table 6).

Fig. 5. Mean stand age for 230 forest stands in DMTNC based on tree age data in 10-year age-classes ($n = 430$).

4.7. Fuel type 1

Fuel type 1 had highest CBD (0.093 kg m^{-3}), litter cover, live (18 m^2 ha^{-1}) and standing dead (2.3 m^2 ha^{-1}) basal area, and live tree density of all fuel types. This group contained 197 kg ha^{-1} of 10 h fuels, 1913 kg ha^{-1} of 100 h fuels, and 7910 kg ha^{-1} of 1000 h fuels (Table 5). While this type did not have the highest 100 and 1000 h fuels, it contained the largest mixture of live and dead fuels. Type 1 fuels were found on sites with low PRR and soil brightness, and high wetness, greenness, and SAVI. SAVI, elevation, and PRR were the three most important predictor variables for this fuel type according to recursive partitioning (Fig. 7).

4.8. Fuel type 2

Fuel type 2 was characterized by high 100 h fuel loads (4342 kg ha^{-1}), intermediate CBD (0.071 kg m^{-2}) and 1000 h fuels (6340 kg ha^{-1}), low log frequencies (11 ha^{-1}), low shrub and litter cover, and few live and standing dead trees (Table 5). Like fuel type 1, the primary carriers of fire were short stature trees and their associated dead and down fuels, although tree cover and fuel loads were higher in this type than in fuel type 1. Type 2 fuels were found on sites with high PRR, brightness and flow accumulation, and low SAVI, wetness, and greenness (Table 6). Mid-infrared reflectance and flow direction were the

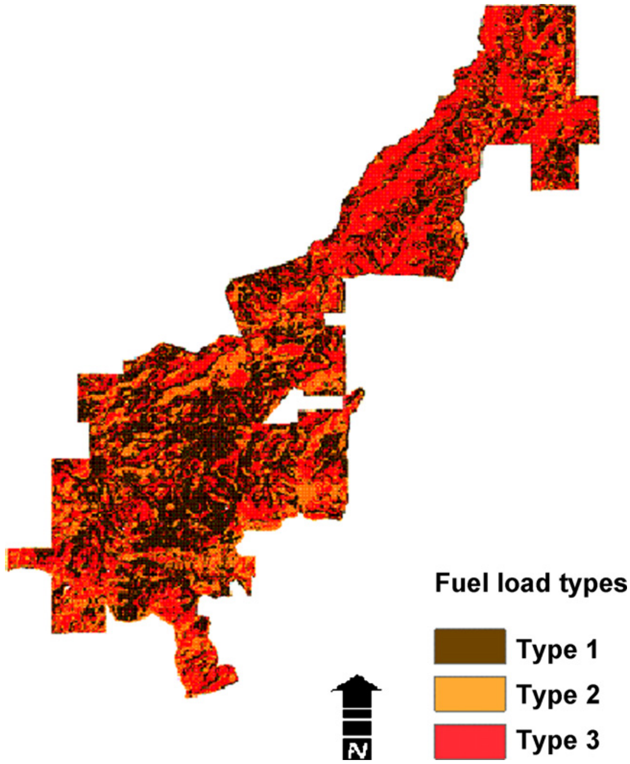

Fig. 6. Fuel map for the Davis Mountains Preserve (TMTNC) developed using recursive partitioning. Fuel types were determined using hierarchical cluster analysis.

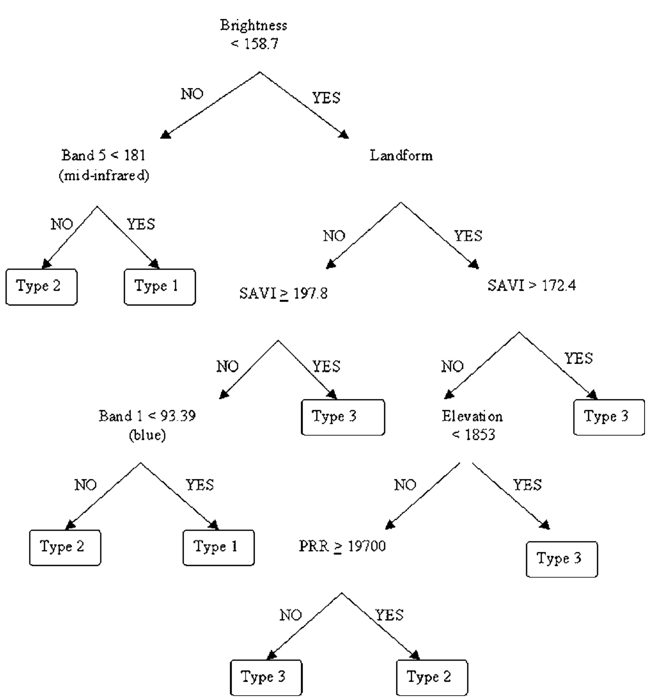

Fig. 7. Classification tree decision rules for fuel types in DMTNC. Fuel types were determined using hierarchical cluster analysis of fuel variables. Predictor variables used in the classification include brightness, bands 1 and 5, landform, soil adjusted vegetation index (SAVI), potential relative radiation (PRR), and flow direction.

Table 6
Mean ± S.E. values of landscape metrics and Landsat ETM+ derived variables for fuel types in DMTNC determined from cluster analysis of fuel variables using relative Euclidean distances and Ward's method

Landscape metrics and Landsat ETM+	1 ($n = 59$)	2 ($n = 79$)	3 ($n = 91$)
Elevation (m)	1775 ± 13.6	1996 ± 203.9	1992 ± 16.6
Slope (°)	21 ± 0.8	19 ± 1.1	16 ± 0.8
PRR**	20411 ± 238.3	19462 ± 254.5	19339 ± 272.9
N aspect	−0.547 ± 0.1	−0.097 ± 0.1	0.791 ± 0.1
S aspect	0.837 ± 0.1	0.087 ± 0.1	0.612 ± 0.1
Topopos 450	−167.52 ± 2.9	1.90 ± 169.6	−3.93 ± 3.4
Topopos 150	−168.81 ± 0.9	0.65 ± 169.5	−0.71 ± 1.0
N flow direction*	−0.15 ± 0.1	−0.12 ± 0.1	0.11 ± 0.1
S flow direction	0.34 ± 0.1	0.12 ± 0.1	0.15 ± 0.1
Flow accumulation	−144 ± 15.1	33 ± 170.1	38 ± 15.8
Topographic configuration	0.11 ± 0.1	0.11 ± 0.2	−0.07 ± 0.1
Band 1***	118 ± 3.9	97 ± 5.5	79 ± 4.8
Band 2	118 ± 3.9	97 ± 5.5	79 ± 4.8
Band 3	107 ± 3.7	86 ± 5.7	67 ± 4.5
Band 4	166 ± 4.9	142 ± 5.8	139 ± 4.7
Band 5	135 ± 4.4	113 ± 5.8	98 ± 5.2
Band 7***	111 ± 3.8	92 ± 5.6	75 ± 4.6
Brightness***	202.5 ± 5.1	206.8 ± 6.7	189.8 ± 5.9
Greeness***	−46.8 ± 3.7	−49.5 ± 6.3	−39.3 ± 4.3
Wetness***	−47.0 ± 4.6	−47.8 ± 6.1	−41.2 ± 5.4
SAVI***	−0.18 ± 4.0	−0.20 ± 6.2	−0.11 ± 4.2

An asterisk (*) marks values that are significant at the $p < 0.001$, and a double asterisk (**) marks values that are significant at the $p < 0.05$ level according to Kruskal–Wallis tests.

primary predictors of type 2 fuels based on recursive partitioning (Fig. 7).

4.9. Fuel type 3

Fuel type 3 contained highest 1000 h fuel loads (10,783 kg ha^{-1}), log frequencies (11 ha^{-1}), and wood volume (14 m^3 ha^{-1}) of all fuel types. However, it was intermediate in all other fuel characteristics including live (11 m^2 ha^{-1}) and standing dead (2.1 m^2 ha^{-1}) BA, CBD (0.069 kg m^{-3}), shrub and litter cover, and live and standing dead tree densities (Table 5). Type 3 fuels were also found on intermediate sites in terms of topography and spectral signature (Table 6, Fig. 7). PRR, flow direction, band 1 (blue), and band 5 (mid-infrared) were the most important predictor variables for this fuel type according to recursive partitioning (Fig. 7).

4.10. Accuracy assessment

Mean overall classification accuracies were 29.1% (range 27.3–36.1%) for the vegetation map, and 29.8 (range 24.5–34.4) for the fuels map (Table 7). Mean Kappa values were 0.55 (range 0.48–0.61) for the vegetation map and 0.54 (range 0.47–0.62) for the fuels map (Table 7). Omission and commission errors for the vegetation and fuels maps were relatively low (Tables 8 and 9).

Table 7
Vegetation and fuel map validation results

	Vegetation map	Fuel map
Misclassification (%)		
Mean	29.1	29.8
Minimum	27.3	24.5
Maximum	36.1	34.4
Kappa (*K*)		
Mean	0.55	0.54
Minimum	0.48	0.47
Maximum	0.61	0.62

Values represent mean, minimum and maximum Kappa statistic (range 0–1) and misclassification rate (%) for 1000 iterations of random data selection. Random data selection was performed by iteratively sub-setting the data 1000 times, using 80% of the data to build the model and 20% of the data to validate the models for each iteration.

5. Discussion

5.1. Forest distribution patterns

The sorting of tree species by elevation, landform, slope, PRR and spectral reflectance in DMTNC is related to intrinsic properties of the vegetation and the physiological ecology of these species in relation to drought and temperature tolerance. Lower elevations of the Southwest are hotter and drier than upper elevations (Barry, 1992). Junipers can tolerate lower predawn and mid-day water potentials and are more resistant to xylem cavitation than pinyon pine (Linton et al., 1998). The dominance of alligator juniper on dry low elevation sites compared to dominance of pinyons on dry mid to high elevation sites in DMTNC and other Southwestern mountains systems is consistent with their physiological capacity to survive and grow in hot, dry conditions.

Although pinyon pines are less drought tolerant than junipers, they are more drought tolerant than upper elevation and valley bottom species such as *P. ponderosa* and *P. strobiformis*. Field and greenhouse drought experiments on pines of the Chiricahua Mountains indicated that pinyon pines survived longer than other pines under persistent drought conditions and they experienced little change in internal water potential, while other pine species experienced a precipitous decline in water potential that was ordered by their elevational distribution (*P. discolor* > *P. leiophylla* > *P. ponderosa*) (Barton and Teeri, 1993). Other research on *P. cembroides* in DMTNC indicated that *P. cembroides* was able to tolerate a wide range of site conditions, making it a site generalist species in comparison to species with more restricted distributions including *P. ponderosa* and *P. strobiformis* (Poulos and Berlyn, in press). This suggests that the distribution of pines in DMTNC is closely related to species' abilities to survive and reproduce across the range of site conditions present in DMTNC.

The species-environment relationships in DMTNC were similar to those reported for other mountain ranges in the Southwest, where elevation, soil moisture, and substrate type were identified as important variables contributing to species' sorting patterns (Whittaker and Niering, 1965, 1968; Wentworth, 1981; White and Vankat, 1993; Barton, 1994). Similarly, we identified elevation as a dominant environmental gradient, but we also found that landform, slope, and PRR were other important predictors of vegetation type in DMTNC.

Differences in the spectral characteristics of the vegetation types in DMTNC were also related to the intrinsic characteristics of the vegetation. High SAVI, greenness, and wetness in MW were the result of dense vegetation in the moist valley bottoms of DMTNC. Similarly, high brightness in oak woodlands corresponded to the abundant grass cover in this savannah-like vegetation type.

Table 8
Confusion matrix for the vegetation map produced for DMTNC via recursive partitioning

Vegetation type	Mesic woodland	Pinyon pine	Gray oak	Alligator juniper	Total	Errors of commission/ producer's accuracy (%)
Mesic woodland	44	13	3	10	70	63
Pinyon pine	11	50	8	3	72	69
Gray oak	2	0	15	2	19	79
Alligator juniper	7	10	1	51	69	74
Total	64	73	27	66		
Errors of omission/user's accuracy (%)	69	68	42	77		

Table 9
Confusion matrix for the fuels map produced for DMTNC via recursive partitioning

Fuel type	1	2	3	Total	Errors of commission/ producer's accuracy (%)
1	33	0	4	37	89
2	18	63	20	101	62
3	8	16	67	91	74
Total	59	79	91		
Errors of omission/user's accuracy (%)	56	42	36		

5.2. Forest stand structure

The high densities of small-diameter trees (≤10 cm DBH) in all vegetation types, coupled with the major recruitment of pines in around 1920 suggests that the current forest structure in DMTNC may be the product of fire exclusion by livestock grazing and favorable climatic conditions after pine germination. A major fire event in occurred in DMTNC 1916 (Poulos, unpublished data), which took place only 3 years prior to the well-recorded recruitment event of ponderosa pine in 1919 in Arizona in response to wetter than normal climatic conditions (Cooper, 1960; White, 1985). 1919 was also an extremely wet year in DMTNC (Poulos, unpublished data), suggesting that the combined effects of the 1916 fire and the 1919 climatic anomaly probably fostered the recruitment and survival of pines at the seedling stage.

The survival of these young trees to adulthood was most likely related to the subsequent drop in fire frequency in DMTNC in the early 1900s. Cattle, sheep, and goat stocking rates were extremely high at the end of the 19th century. During this era high stocking rates ranging from 4.1 to 12.3 acres/animal unit were typical in west Texas, compared to present day stocking of 75–200+ acres/animal unit (Downey, 1978; Clayton, 1993). Such high stocking rates are thought to effect forests by removing the fine fuels necessary for fire ignition and spread (Leopold, 1924; Arnold, 1950). High stocking rates were typical of ranchlands across the western United States in the late 1800s and early 1900s, and they are generally considered a major cause of the cessation of fire in the early 1900s in the West that probably triggered large-scale tree recruitment pulses after the cessation of fire (Cooper, 1960).

The high density of small diameter trees across in DMTNC corresponds to the recent tree recruitment patterns observed in other fire-excluded sites in the southwestern United States. Stand densities in DMTNC were most similar to those observed in the Guadalupe Mountains, only 150 miles to the north (Sakulich and Taylor, 2007), where mixed conifer forests (MW in this study) also had tree densities of over 1500 stems ha^{-1}. While densities were similar in mixed conifer forests, DMTNC had much higher tree densities than the Guadalupe Mountains in pinyon and juniper dominated vegetation types. Tree densities in DMTNC were also similar to the fire-suppressed mixed conifer forests in the Camp Navajo Army National Guard Base and in the San Francisco Peaks of Arizona, which had 1436 and 1613 stems ha^{-1}, respectively (Fulé et al., 1997; Heinlein et al., 2005).

The differences between conifer and oak diameter distributions in DMTNC were probably related to species life history. Ponderosa pine, southwestern white pine, pinyon pine and alligator juniper all regenerate readily via seed within 10–20 years after fire (Krugman and Jenkinson, 1974; Sackett, 1984). In contrast, major oak recruitment events occur through post-fire sprouting in the Southwest, with some regeneration occurring via seed in the absence of fire (Keeley, 1992; Barton, 1999). This suggests that that the high densities of intermediate sized oaks in DMTNC may have been a remnant of post-fire sprouting of oaks following the last major fire event in DMTNC.

5.3. Fuel accumulation patterns

Our results suggested that the distribution of larger fuels across dissected landscapes was closely associated with some of the same factors that influenced the distribution of vegetation, although the mechanisms responsible for these patterns were not identical. The differences between the vegetation and fuels maps highlight that fuel loads were not directly related to vegetation types, reinforcing the claim by Keane et al. (2001) that vegetation maps should not be used as the sole basis for fuels mapping.

In general, higher productivity sites existed at high elevations in response to more favorable climatic conditions with increasing elevation (Barry, 1992). The pattern of high fuel accumulation in high productivity sites in DMTNC is consistent with research in other parts of the western U.S., where forests on high productivity sites averaged more pieces and volume ha^{-1} of down wood than low productivity sites (Harmon et al., 1986; Spies et al., 1988).

The topographic effects on fuel distribution patterns were similar to those for vegetation, but the relationship between topographic position and gravity underscored the pattern of fuel heavy fuel loads in valley bottoms and low fuel loads on mid-slopes and ridgetops. The fact that mesic valley bottoms are more productive than mid-slopes that receive high amounts of incident solar radiation partially explains the trend of higher fuel loads on lower topographic positions. Valley bottoms also receive sedimentation from upland areas during rainstorms, and fuels often settle in lower topographic positions by rolling down hill from middle and upper topographic positions. Likewise, steeper slopes contain lower amounts of fuel because they wash downward to flatter areas. The combined effects of higher site productivity, fuel accumulation from upslope outwash and gravity, and *in situ* fuel contributions from vegetation in valley bottoms potentially explain why fuel loads were highest in lower topographic positions in our study. These patterns are consistent with the limited body of work that has examined the relationships between the distribution of fuels and topography (Rubino and McCarthy, 2003; Graham and McCarthy, 2006). However, our work presents new information about the distribution of larger fuels at the landscape-scale in the southwestern United States that can be used to help managers target locations on the landscape that are in most need of fuel reduction treatments.

The high density of small trees and the CBD of vegetation in DMTNC were direct measures of the amount of live fuels that could potentially carry a fire across the landscape and serve as ladder fuels to move a fire from the forest floor to the canopy. Live fuels are high in the Southwest due to recent increases in tree recruitment in the absence of frequent, low intensity fire. Contemporary forest stand structures in DMTNC are quite different from the open, park-like forests that are thought to have dominated the Southwest prior to grazing and fire suppression (Cooper, 1960). Recent changes in fuel loads increase the risk of severe, high intensity fires that are dramatically different from historically frequent, low intensity fire regimes.

Our findings in DMTNC were consistent with live fuel loads in the Huachuca Mountains of southeastern Arizona (Miller et al., 2003) and in the Grand Canyon (Fulé et al., 2004). CBD estimates in DMTNC were also similar to other pinyon-juniper and ponderosa pine forests in the Mogollon Rim (Hampton et al., 2003) ranging between 0.05 and 0.1 kg m^{-3}, but were intermediate compared to more mesic upland forests of Idaho (Falkowski et al., 2005) and Washington (Wimberly et al., 2003) which can be higher than 0.15 kg m^{-3}.

Standing dead and dead and down fuels in DMTNC corresponded closely to fuel loads reported for other fire-suppressed sites in the Southwest, suggesting that these forests are susceptible to future high intensity fire. Sackett (1979) reported an average of 7.8 tonnes/acre of large woody fuels in northern Arizona and Harrington (1982) reported an average of 4 tonnes/acre in open old growth forests and 10 tonnes/acre in closed, overstocked forests in southeastern Arizona. Type 2 fuels in DMTNC corresponded closely to the fuel loads of larger fuels in open forests in Harrington's (1982) study, and type 3 fuels were similar to his closed forest fuel loads. Large diameter fuels in DMTNC were also similar to more recent work in pinyon–juniper and oak savanna woodlands by Miller et al. (2003) and Sanchez-Flores and Yool (2004), and the low fuel loadings of fuel type 1 corresponded closely to the open juniper and oak savannas studied by Miller et al. (2003).

Our misclassification rates of approximately 30% were typical of other vegetation mapping projects that used decision tree classifiers. Other overall misclassification rates for predicting vegetation and fuels using classification tree and biophysical gradient models ranged from 11% to 33% (Franklin, 1998, 2002; Miller et al., 2003; Brown de Colstoun et al., 2003; Falkowski et al., 2005). The misclassification rates near 30% reflected the difficulty of reducing ecological processes like species distribution and fuel accumulation patterns to numerical models. Moreover, our project mapped distinct vegetation assemblages at the species level, rather than the majority of vegetation mapping studies that assign vegetation types to broader categories such as oak, grassland, or conifer cover types. Spectral confusion from overlap in species composition among vegetation types probably explains the error rates in our study, especially since species like juniper and pinyon pine were distributed across multiple vegetation types. For example, all vegetation types contained some pinyon pine, alligator juniper, and gray oak, which made it difficult to differentiate between classes containing different densities of these species. GO forests had the lowest user accuracy of all groups, probably because they were spectrally similar to PP forests, and were found on similar sites. MW had the lowest producer's accuracy, which was also potentially related to the fact that this forest cover type contained the highest species richness of all vegetation types, and therefore had high potential confusion with other types. The fuel decision tree also performed well for predicting fuel loads across the landscape of DMTNC. Some confusion did occur between fuel types, which was probably also due to overlap in the spectral signature of live fuels and environmental site characteristics.

6. Conclusion

The results from this study provided decision support tools for the mitigation of fire hazards and the restoration of forest vegetation to its pre-fire suppression state. The integrated classification tree approach applied to this study proved to be an effective tool for quantifying vegetation and fuel abundance and distribution patterns and for predicting them across the landscape of DMTNC. Our combined use of detailed field data, biophysical gradient modeling, and remotely sensed spectral information provided detailed information about the factors that governed the abundance of vegetation, forest stand structure, and the accumulation of fuels in DMTNC. Furthermore, we believe that the methods applied to this study could be applied to other regions of the Southwest where detailed forest and fuel inventory data are lacking.

The information provided by this study can be used for a range of forest and fire management activities, although restoration of vegetation and fuels to conditions that resemble pre-fire suppression conditions may not be a feasible goal on all forestlands. Nature Conservancy managers in DMTNC are committed to maintaining ecosystem structure and function through active management (i.e. forest thinning and prescribed burning). Our results provided baseline information about recent changes in forest stand structure, and the abundance and distribution patterns of vegetation and fuels in DMTNC, which can be used to target high-risk areas on the landscape for tree density and fuel reduction treatments using thinning and prescribed fire. Outputs from our work can also be input into forest simulation programs including the fire effects module of FVS (Crookston, 1997) and Landscape Management Software (LMS) (Carey et al., 1996), which could be used for planning and implementation of vegetation and fuel restoration treatments.

Acknowledgements

We wish to thank The Davis Mountains Preserve of The Nature Conservancy of Texas for logistical support for this project. Larry Bonneau of the Yale Center of Earth Observation was instrumental in generating the fuels and vegetation maps for this project. We also thank Dr. Shelley Danzer of the Fort Huachuca Army National Guard Base and two anonymous reviewers for comments on earlier drafts of this manuscript. Funding for this research was graciously provided by the Joint Fire Sciences Program of the Department of the Interior (# 03-3-3-13).

References

Appelquist, M.B., 1958. A simple pith locator for use with off-centered increment cores. J. For. 56, 141.

Arnold, J.F., 1950. Changes in ponderosa pine-bunchgrass ranges in Arizona resulting from pine regeneration and grazing. J. For. 48, 118–126.

Barry, R.B., 1992. Mountain Weather and Climate. Meitheuen, London.
Barton, A.M., 1994. Gradient analysis of relationships among fire, environment and vegetation in a southwestern USA mountain range. Bull. Torrey Bot. Club 121, 251–265.
Barton, A.M., 1999. Pines versus oaks: effects of fire on the composition of Madrean forests in Arizona. For. Ecol. Manage. 120, 143–156.
Barton, A.M., Teeri, J.A., 1993. The ecology of elevational positions in plants: drought resistance in five montane pine species in southeastern Arizona. Am. J. Bot. 80, 15–25.
Beers, T.W., Dress, P.E., Wensel, L.C., 1966. Aspect transformation in site productivity research. J. For. 64, 691–692.
Biswell, H.H., Kallander, H.R., Komarek, R., Vogl, R.J., Waver, H., 1973. Ponderosa pine management. Tall timbers Res. Stn. Misc. Pub. No. 2. Tall Timbers Research Station, Tallahassee, FL, p. 49.
Bowmar, G.W., 1995. Texas Weather. University of Texas Press, Austin.
Breiman, L., Freidman, J.H., Olshen, R.A., Stone, C.J., 1984. Classification and Regression Trees. Wadsworth, Belomont, CA.
Brisette, J.C., Ducey, M.J., Gove, J.H., 2003. A field test of point relascope sampling of down coarse woody material in managed stands in the Acadian forest. J. Tor. Bot. Soc. 130, 79–88.
Brown, D.G., 1994. Predicting vegetation types at treeline using topography and biophysical disturbance variables. J. Veg. Sci. 5, 641–656.
Brown, J.K., 1974. Handbook for inventorying downed woody material. USDA For. Ser., Intermountain Res. Stn., Ogden, UT, Gen. Tech. Rep. INT-16.
Brown, J.K., Oberheu, R.D., Johnston, C.M., 1982. Handbook for inventorying surface fuels and biomass in the Interior West. USDA For. Ser., Intermountain Res. Stn., Ogden, UT, Gen. Tech. Rep. INT-129.
Brown de Colstoun, E.C., Story, M.H., Thompson, C., Commisso, K., Smith, T.G., Irons, J.R., 2003. National park vegetation mapping using multitemporal Landsat 7 data and a decision tree classifier. Rem. Sens. Environ. 85, 316–327.
Byram, G.M., 1963. An analysis of the drying process in forest fuel material. In: Presentation at International Symposium on Humidity and Moisture. Washington, DC 38 pp.
Carey, A.B., Elliott, C., Lippke, B.R., Sessions, J., Chambers, C.J., Oliver, C.D., Franklin, J.F., Raphael, M.G., 1996. Washington Forest Landscape Management Project—A pragmatic ecological approach to small-landscape management. Report No. 2, Washington State Dep. Nat. Res., Washington Forest Landscape Management Project.
Clayton, L., 1993. Historic Ranches of Texas. University of Texas, Austin.
Congalton, R.G., Green, K., 1999. Assessing the Accuracy of Remotely Sensed Data: Principles and Practices. Lewis, New York.
Cooper, C.F., 1960. Changes in vegetation, structure, and old growth of southwestern pine forests since white settlement. Ecol. Monogr. 30, 129–164.
Crookston, N.L., 1997. Suppose: an interface to the forest vegetation simulator. In: Teck, R., Moeur, M., Adams, J. (Eds.), Proceeding: Forest Vegetation Simulator Conference, February 3–7, 1997, Fort Collins, CO. USDA For. Ser., Intermountain Res. Stn., Ogden, UT, Gen. Tech. Rep. INT-373.
De'ath, G., Fabricius, K.E., 2000. Classification and regression trees: a powerful yet simple technique for ecological data analysis. Ecology 8, 3178–3192.
Delta-T Devices, 1999. HemiView Canopy Analysis Software Version 2.1.
Downey, A.E., 1978. Terrell County, Texas, its past–its people. Rangel Printing, San Angelo.
Dufrêne, M., Legendre, P., 1997. Species assemblages and indicator species: the need for a flexible asymmetrical approach. Ecol. Monogr. 67, 345–366.
ESRI ArcMap Version 9.1, 2005. ESRI Inc., Redlands, CA.
Falkowski, M.J., Gessler, P.E., Morgan, P., Hudak, A.T., Smith, A.M.S., 2005. Characterizing and mapping forest fire fuels using ASTER imagery and gradient modeling. For. Ecol. Manage. 217, 129–146.
Faulk, O.B., 1970. Arizona: A Short History. University of Oklahoma Press, Norman, Oklahoma, p. 266.
Fosberg, M.A., Deeming, J.E., 1971. Derivation of the 1- and 10-hour timelag fuel moisture calculations for fire-danger rating. U.S. Dep. Agric. For. Serv. Res. Note RM-207, Ft. Collins, CO.
Franklin, J., 1998. Predicting the distribution of shrub species in southern California from climate and terrain-derived variables. J. Veg. Sci. 9, 733–748.
Franklin, J., 2002. Enhancing a regional vegetation map with predictive models of dominant plant species in chaparral. J. Veg. Sci. 5, 135–146.
Fulé, P.Z., Covington, W.W., Moore, M.M., 1997. Determining reference conditions for ecosystem management of southwestern ponderosa pine forests. Ecol. Appl. 7, 895–908.
Fulé, P.Z., Covington, W.W., Moore, M.M., Heinlein, T.A., 2002. Natural variability in forests of the Grand Canyon, USA. J. Biogeog. 29, 31–47.
Fulé, P.Z., Crouse, J.E., Cocke, A.E., Moore, M.M., Covington, W.W., 2004. Changes in canopy fuels and potential fire behavior 1880–2040: Grand Canyon, Arizona. Ecol. Model. 175, 231–248.
Gilabert, M.A.J., Gonzalez-Piqueras, J., Garcia-Haro, F.J., Melia, J., 2002. A generalized soil-adjusted vegetation index. Rem. Sens. Environ. 82, 303–310.
Gopal, S., Woodcock, C.E., 1996. Remote sensing of forest change using artificial neural networks IEEE Transactions of Geoscience. Rem. Sens. 34, 398–404.
Gove, J.H., Ducey, M.J., Stahl, G., Ringvall, A., 2001. Point relascope sampling: a new way to assess downed coarse woody debris. J. For. 99, 4–11.
Graham, J.B., McCarthy, B.C., 2006. Forest floor fuel dynamics in mixed-oak forests of south-eastern Ohio. Int. J. Wildland Fire 15, 1–10.
Hampton, H.M., Xu, Y., Prather, J.W., Aumack, E.N., Dickson, B.G., Howe, M.M., Sisk, T.D., 2003. Spatial tools for guiding forest restoration and fuel reduction efforts. In: Proceedings of the 2003 ESRI Users Conference. San Diego, CA (CD-ROM).
Harmon, M.E., Franklin, J.F., Swanson, F.J., Sollings, P., Grgory, S.V., Lattin, J.D., Anderson, N.H., Cline, S.P., Dume, N.G., Sedell, J.R., Lienkaemper, G.W., Cromack, K., Cummum, K.W., 1986. Ecology of coarse woody debris in temperate ecosystems. Adv. Ecol. Res. 15, 133–302.
Harrington, M.G., 1982. Stand, fuel, and potential behavior characteristics in an irregular southeastern Arizona ponderosa pine stand. USDA For. Ser., Intermountain Research Station, Fort Collins, CO, Note RM-418.
Heinlein, T.A., Moore, M.M., Fulé, P.Z., Covington, W.W., 2005. Fire history and stand structure of two ponderosa pine-mixed conifer sites: San Francisco Peaks, Arizona, USA. Int. J. Wildland Fire 14, 307–320.
Hinckley, L.C., 1944. The vegetation of the Mount Livermore area in Texas. Am. Mid. Nat. 32, 236–250.
Huete, R.A., 1988. A soil-adjusted vegetation index (SAVI). Rem. Sens. Environ. 25, 295–309.
Jordan, G.J., Ducey, M.J., Gove, J.H., 2004. Comparing line-intersect, fixed-area, and point relascope sampling for dead and downed coarse woody material in a managed northern hardwood forest. Can. J. For. Res. 34, 1766–1775.
Kauth, R.J., Thomas, G.S., 1976. The tasseled cap—a graphic description of the spectral–temporal development of agricultural crops seen by Landsat. In: Proceedings of the Symposium on Machine Processing of Remotely Sensed Data. Perdue University, West Lafayette, Indiana pp. 4B-41–4B-50.
Keane, R.E., McNicoll, C.H., Schmidt, K.M., Garner, J.L., 1997. Spatially explicit ecological inventories for ecosystem management planning using gradient modeling and remote sensing. In: Proceedings of the Sixth Forest Service Remote Sensing Applications Conference—Remote Sensing; People in Partnership with Technology. American Society of Photogrammetry and Remote Sensing, Bethesda, MD, 448 pp, pp. 135–146.
Keane, R.E., Burgan, R., vanWagtendonk, J., 2001. Mapping wildland fuels for fire management across multiple scales: integrating remote sensing, GIS, and biophysical modeling. Int. J. Wildland Fire 10, 301–319.
Keane, R.E., Mincemoyer, S.A., Schmidt, K.A., Long, D.G., Garner, J.L., 2000. Mapping vegetation and fuels for fire management on the Gila National Forest Complex, New Mexico. USDA For. Ser., Intermountain Research Station, Ogden, UT, Gen. Tech. Rep. RMRS-46-CD.
Keane, R.E., Reinhardt, E.D., Scott, J., Gray, K., Reardon, J., 2005. Estimating forest canopy bulk density using six indirect methods. Can. J. For. Res. 35, 724–739.
Keeley, J.E., 1992. Recruitment of seedlings and vegetative sprouts in unburned chaparral. Ecology 73, 1194–1208.
Kessell, S.R., 1976. Gradient modeling: a new approach to fire modeling and wilderness resource management. Environ. Manage. 1, 39–48.
Krugman, S.L., Jenkinson, J.L., 1974. Pinus L. pine. In: Schopmeyer, C.S. (tech. coord.) Seeds of Woody Plants in the United States. Agric. Handb. 450. USDA, For. Serv., Washington, D.C., pp. 598–638.

Kruskal, W.H., Wallis, W.A., 1952. Use of ranks in one-criterion variance analysis. J. Am. Stat. Assoc. 47, 583–621.

Leopold, A., 1924. Grass, brush, timber and fire in southern Arizona. J. For. 22, 1–10.

Lewis, M.M., 1998. Numerical classification as an aid to spectral mapping of vegetation communities. Plant Ecol. 136, 133–149.

Linton, M.J., Sperry, J.S., Williams, D.G., 1998. Limits to water transport in *Juniperus osteosperma* and *Pinus edulis*: implications for drought tolerance and regulation of transpiration. Funct. Ecol. 12, 906–911.

Maingi, J.K., Ffolliot, P.F., 1992. Specific gravity and estimated physical properties of emory oak in southeastern Arizona. In: Folliot, P.F., Gottfried, G.J., Bennett, D.A., Hernandez, V.M., Ortega-Rubio, A. (Eds.), Ecology and Management of Oak and Associated Woodlands: Perspectives in the Southwestern US and Northern Mexico. USDA For. Ser., Fort Collins, RM-218.

McCune, B., Mefford, M.J., 1999. PC-ORD. Multivariate Analysis of Ecological Data, Version 4. MJM Software Design, Gleneden Beach, Oregon.

McCune, B., Grace, J.B., 2002. Analysis of Ecological Communities. MJM Software Designs, Gleneden Beach, Oregon.

Miller, J.D., Danzer, S.R., Watts, J.M., Stone, S., Yool, S.R., 2003. Cluster analysis of structural stage classes to map wildland fuels in a Madrean ecosystem. J. Environ. Manage. 68, 239–252.

Minasny, B., McBratney, A.B., 1999. FuzME version 1.0. In: Australian Centre for Precision Agriculture, The University of Sydney.

Minitab Incorporated, 1999. Minitab for Windows, Version 12.2. Minitab Incorporated, State College, PA.

Moeur, M., Riemann, J., Hershey, R., 1999. Preserving spatial and attribute correlation in the interpolation of forest inventory data. In: Lowell, K., Jaton, A. (Eds.), Spatial Accuracy Assessment: Land Information Uncertainty in Natural Resources. Ann Arbor Press, Chelsea, Michigan.

Moore, M.M., Huffman, D.W., Fulé, P.Z., Covington, W.W., Crouse, J.E., 2004. Comparison of historical and contemporary forest structure and composition on permanent plots in southwestern ponderosa pine forests. For. Sci. 50, 162–176.

Ohmann, J.L., Gregory, M.J., 2002. Predictive mapping of forest composition and structure with direct gradient analysis and nearest neighbor imputation in coastal Oregon, U.S.A. Can. J. For. Res. 32, 725–741.

Ohmann, J.L., Spies, T.A., 1998. Regional gradient analysis and spatial pattern of woody plant communities of Oregon forests. Ecol. Monogr. 68, 151–182.

Ohmann, J.L., Spies, T.A., Gregory, M.J., in press. Influences of environment, disturbance, and ownership on forest vegetation biodiversity in coastal Oregon, USA. Ecol. Appl.

Pierce, K.B., Lookingbill, T., Urban, D., 2005. A simple method for estimating potential relative radiation (PRR) for landscape-scale vegetation analysis. Landsc. Ecol. 20, 137–147.

Poulos, H.M., Berlyn, G.P., in press. Phenotypic plasticity in needle morphology and water status of *Pinus cembroides* across an elevational gradient in the Davis Mountains of west Texas, USA. J. Torr. Bot. Soc.

R Development Core Team, 2005. A language and environment for statistical computing. R Foundation for Statistical Computing, Vienna, Austria. Available [online] at: http://www.r-project.org (accessed October10, 2005).

Research Systems Inc., 2005. ENVI Version 4.2. Research Systems Inc., Boulder, CO.

Rubino, D.L., McCarthy, B.C., 2003. Evaluation of coarse woody debris and forest vegetation across topographic gradients in a southern Ohio forest. For. Ecol. Manage. 183, 221–238.

Sackett, S.S., 1979. Natural fuel loadings in ponderosa pine and mixed conifer forests of the Southwest. USDA For. Ser., Intermountain Res. Stn., Fort Collins, CO, RMRS-213.

Sackett, S.S., 1984. Observations on natural regeneration in ponderosa pine following a prescribed fire in Arizona. USDA For. Ser., Rocky Mountain Forest and Range Exp. Stn., Fort Collins, CO, Res. Note RM-435.

Sakulich, J., Taylor, A.H., 2007. Fire regimes and forest structure in a sky island mixed conifer forest, Guadalupe Mountains National Park, Texas. USA. For. Ecol. Manage. 241, 62–73.

Sanchez-Flores, E., Yool, S.R., 2004. Site environment characterization of downed woody fuels in the Rincon Mountains, Arizona: regression tree approach. Int. J. Wildland Fire 13, 467–477.

Spies, T.A., Franklin, J.F., Thomas, T.B., 1988. Coarse woody debris in Douglas fir forests of western Oregon and Washington. Ecology 69, 1689–1702.

Stokes, M.A., Smiley, T.A., 1968. An Introduction to Tree Ring Dating. University of Chicago Press, Chicago.

Swetnam, T.W., Baisan, C.H., 1996. Historical fire regime patterns in the southwestern United States since AD 1700. In: Allen, C.D. (Ed.), Proceedings of the Second La Mesa Fire Symposium. USDA For. Ser. Gen. Tech. Rep. RM-GTR-286, pp. 11–32.

Turner, A.J., 1977. Soil Survey of Jeff Davis County. USDA, Soil conservation Service, Texas.

USDA and USDI [USDA Forest Service, and U.S. Department of the Interior], 2000. National fire plan: managing the impacts of wildfires on communities and the environment. A report to the president in response to the wildfires of 2000 [online, URL: {http://www.firepplan.gov}].

US Geological Survey, 2005. National Elevation Dataset. US Geol. Survey, Sioux Falls, SD.

Wentworth, T.R., 1981. Vegetation on limestone and granite in the Mule Mountains, Arizona. Ecology 62, 469–482.

White, A.S., 1985. Presettlement regeneration patterns in a southwestern ponderosa pine stand. Ecology 71, 2060–2068.

White, M.A., Vankat, J.L., 1993. Middle and high-elevation coniferous forest communities of the North Rim Region of Grand-Canyon National Park, Arizona, USA. Vegetatio 109, 161–174.

Whittaker, R.H., Niering, W.A., 1965. Vegetation of the Santa Catalina Mountains, Arizona. II. A gradient analysis of the south slope. Ecology 46, 429–452.

Whittaker, R.H., Niering, W.A., 1968. Vegetation of the Santa Catalina Mountains, Arizona. IV. Limestone and acid soils. J. Ecol. 56, 523–544.

Wimberly, M.C., Ohman, J.L., Pierce, K.B., Gregory, M.J., Fried, J.S., 2003. A multivariate approach to mapping forest vegetation and fuels using GIS databases, satellite imagery, and forest inventory plots. In: Proceedings of the Second International Wildland Fire Ecology and Fire Management Congress, November 16–20, 2003, American Meteorological Society, Orlando, FL.